TRANSFER PROCESSES IN HEAVY ION REACTIONS

G. Pollarolo

Dipartimento di Fisica Teorica, Università di Torino and
Istituto Nazionale di Fisica Nucleare, Sezione di Torino, Torino, Italy

The basic properties of transfer reactions will be summarized and, by employing a semiclassical model, I will try to demonstrate their relevance for the understanding of the reaction mechanism. In particular I will focus on the calculations of the quasi-elastic excitation functions, on the discussion of multinucleon transfer reactions measured with the PRISMA-CLARA set up and I will show that these reactions may lead to the production of heavy neutron rich nuclei.

1. Introduction

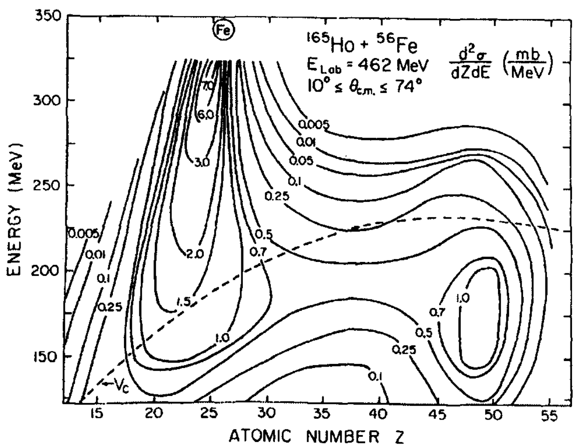

Fig. 1. Double differential cross section for the ^{56}Fe + ^{165}Ho reaction. The dash-line corresponds to the Coulomb barrier of two touching spheres. The fact that a large fraction of the yields lies below this line indicates that the fragments separate with large deformations.

Transfer reactions play an essential role in nuclear physics, both for the understanding of the nuclear structure and for the modelling of the dynamics of a collision process. Here I will discuss mostly the aspects relevant for the dynamics and, to this purpose, I find convenient to start my contribution with a short introduction on the main characteristics of a heavy ion collisions. One illustrative example is shown in Fig. 1 where the yields of the reaction are plotted as a function of the charge and total kinetic energy of the detected fragments. Here one can clearly recognize two components: a ridge that from the entrance channel extends to very low energies and a broad peak at very low energies and with charges compatible with a fusion-fission process. The ridge component contains most of the reaction cross section and it is compatible with transfer reactions and evaporation processes. Here I remind that for stable nuclei only proton stripping and neutron pick-up reactions are allowed from optimum *Q*-value. The broad peak component cannot be ascribed to a complete fusion process, i.e. to the formation of a compound nucleus, in fact its average angular momentum is much larger than the one that can be substained by the nucleus as has been estimated from the liquid drop model. More properly one should here talk about a capture process leading to the formation of a di-nuclear complex that will separate afterword.

From the broadening of the charge distribution as a function of dissipated energy one got inspiration for the development of models that describe the exchange of mass and charge with transport equations and that introduce frictional forces [1] for the dissipation of energy and angular momentum. The microscopic origins of the frictional force, of the drift and diffusion coefficients are usually attributed to transfer processes. For the frictional force a commonly used expression is the so called wall-formula that is derived from a one-body theory [2]. In this model the dissipation of energy is caused by the collision of nucleons against the wall of the mean field. The nature and the *r*-dependence of these forces are still the object of several investigations since their role is quite important in processes like fusion and fission.

In this contribution I am not so much interested in the discussion of this problematic but I will try to analyze the data with a model that incorporate explicitly the surface degree of freedom (important for the treatment of the large deformation that may occur in the collision) and transfer degrees of freedom. The excitation of these last degrees of freedom is obtained by using the actual formfactors for the transfer of one nucleon (neutron and proton, stripping and pick-up). Multinucleon transfer is here treated in the successive approximation. After a very short introduction of the model I will try to summarize some applications of the model to the study of multinucleon transfer reactions and to quasi-elastic barrier distributions. Toward the end I will apply the above model to show that multinucleon transfer reactions can provide an important mechanism for the production on neutron rich nuclei in the region just below the lead, i.e. in the region of the *N*=126 shell closure.

2. The model

By exploiting the very short wave length of the relative motion, one can use semi-classical arguments to develop reaction models that treat classically the relative motion and incorporate couplings to the intrinsic degrees of freedom of projectile and target. In the model I am going to use, these degrees of freedom are identified with the isoscalar surface modes (low lying and high-lying states) and the exchange of nucleons. The relevance of the surface degrees of freedom is particularly evident in fusion reactions where it has been shown that these couplings [3] account for most of the missing cross section. For these reactions the effect of the couplings preclude us from talking about a single barrier but it is more convenient to talk about a distribution of barriers (several MeV wide) [4]. The importance of transfer reactions, i.e. of couplings to single-particle degrees of freedom, in the description of a heavy-ion reaction has been underlined in several papers [5 - 7]. These transfer degrees of freedom are weak, very numerous and span a wide range of Q-values. They are governed by long range formfactors and are providing the main contribution to the absorptive and polarization potential and for the frictional force.

The GRAZING model will not be summarized here, for details refer to the works in Refs. [8 - 10], here suffices to remember that the cross section are calculated by solving in an approximate way the well known system of coupled equations

$$i\hbar\dot{c}_{\beta}(t)=\sum_{\alpha}c_{\alpha}(t)\langle\beta|H_{\mathrm{int}}|\alpha\rangle e^{\frac{i}{\hbar}(E_{\beta}-E_{\alpha})t+i(\delta_{\beta}-\delta_{\alpha})} \tag{1}$$

obtained from the time dependent Schrödinger equation

$$i\hbar\dot{\Psi}(t)=(H_0+H_{\mathrm{int}})\ \Psi(t) \tag{2}$$

by expanding the total wave function of the system in terms of channel wave functions $\Psi_{\alpha}=\Psi^{\alpha}(t)\Psi^{A}(t)e^{i\delta(\vec{R})}$ corresponding to the states of the asymptotic mass partitions. The coefficient c_β gives the amplitude for the system to be in channel β.

The residual interaction H_{int} is constructed by using the well known form-factors for the inelastic excitation and for the transfer of one-nucleon (neutron and proton, stripping and pick-up). Multi-nucleon transfer is included in the successive approximation. The time dependence of the interaction is obtained by solving the classical equations of motion in a nuclear plus Coulomb field. For the nuclear potential it is used the simple Wood Saxon parametrization [12] whose parameters come from the knowledge of the nuclear densities and have been slightly adjusted through a systematic comparison of elastic scattering data.

Since we are expanding the total wave function of the system in terms of the different states of the asymptotic mass partitions we will be able to describe only the ridge component of the final yields. For the broad peak the model is only able to estimate the capture cross section, the tunneling trough the barrier is estimated via the parabolic approximation.

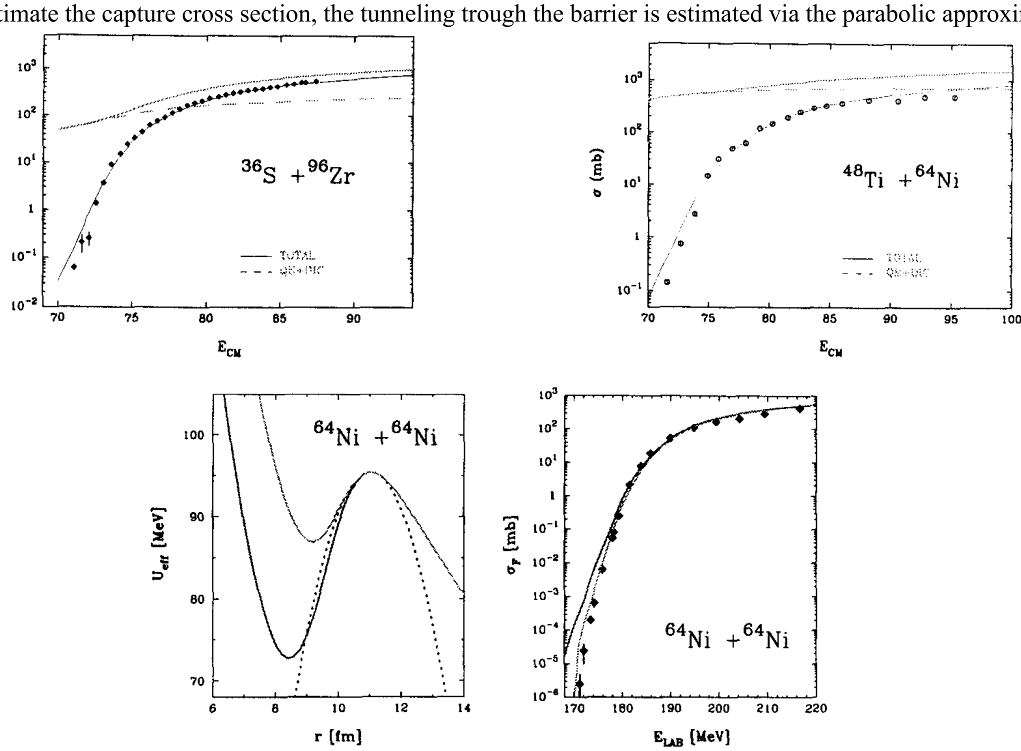

Fig. 2. (Top row) It is shown the calculated capture cross sections in comparison with the data, also shown are total reaction (thick line) and the total binary cross sections (dashed-line). (bottom row) For the $^{64}Ni+^{64}Ni$ system are shown the potentials (left) and the corresponding fusion cross sections (right) in comparison with the experimental data. The potential with the deeper pocket corresponds to the folding potential of Ref. [12]. The shallower one is the one that reproduce the fusion at very low energy (fusion hindrance).

In Fig. 2 (top row) are shown, for the indicated systems, the comparisons of the estimated capture cross sections with fusion data. In the same figure are also shown the reaction and direct (quasi-elastic and deep-inelastic) total cross sections. In the low energy region the direct component dominates the reaction for all systems. The same model has also been used to show that the fusion cross section at very low energy is sensitive to the position of the internal pocket of the potential. To do so one relaxed the parabolic approximation in the calculation of the tunneling through the barrier by using the more appropriate WKB approximation. An example of such calculation is shown in bottom row of Fig. 2 where for the indicated system are displayed the r-dependence of the potential with the extracted capture cross section in comparison with the experimental data. From this consideration on the fusion cross section it is clear that the empirical potential of Ref. [12] describes adequately the relative motion of the two ions and provides the correct matrix elements (the nuclear component) for the couplings of the surface modes.

The component of the interaction *Hint*, responsible for the exchange of nucleons, is constructed from the one-particle transfer formfactors calculated by using the parametrization of Ref. [13]. To show that the model provide a good description of grazing reactions we analyze the ^{58}Ni + ^{124}Sn system. This is one of the few systems for which we have complete measurements of all reaction channels in a wide energy range [14, 15, 16, 17, 18, 19, 20, 21, 22] and for which a coupled channels analysis [23], that includes inelastic and transfer channels, has been performed. From Fig. 3 is clear that the model gives, for all energies, a good description of the elastic angular distributions (first column), of the angular distributions for the inclusive cross sections of one-neutron pick-up, of one-proton stripping channels and of some multi-neutrons transfer channels (last three columns). In the case of elastic scattering the good description shown by the full line is obtained by adding to the true elastic (shown with a dash-line) all the inelastic channels. The shown results are very similar to the one obtained in Ref. [23] where quantum mechanical coupled-channels formalism has been used.

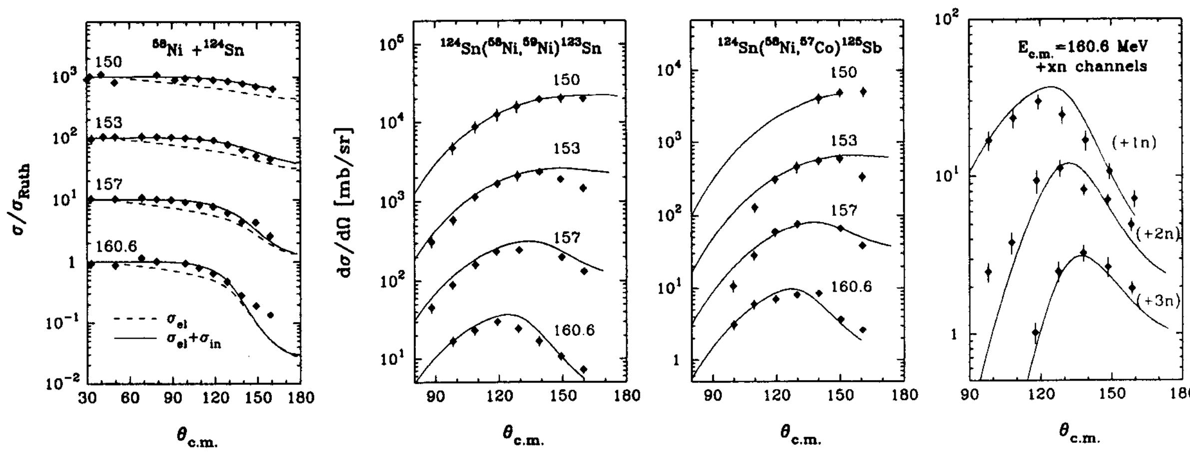

Fig. 3. In the first column is shown the ratio to Rutherford of the elastic plus inelastic scattering (full line) in comparison with the experimental data. The pure elastic scattering (dash-line) is also shown. The following two columns display the calculated angular distributions of the inclusive one-neutron pick-up and one-proton stripping channels. The last column displays the angular distributions for some multi-neutron transfer channels at the indicated bombarding energy.

Another interesting application is provided by the calculation of the quasi-elastic (*QE*) excitation functions, these can provide complementary information on the barrier distributions for heavy system that can not lead to fusion because of the large Coulomb repulsion.

Detailed measurements of *QE*-excitation function can be found in Ref. [24]. The model has been used to construct these excitation functions by calculating the angular distribution of all *QE*-channels in step of 1 MeV of bombarding energy and summing their contributions at θ_{lab} = 172º. For all analyzed systems the *QE*-excitation functions are displayed in the top row of Fig. 4. The barrier distributions $B(E)$ obtained from the excitation functions with a three-point formula energy derivative, are shown in the central row. The points represent the experimental data of Ref. [24]. Both barrier distributions and excitation functions are very well described by the theory. Interpreting the centroid of the barrier distributions as the position of the effective barrier E_B^{eff} one sees that the couplings give rise to a lowering of the Coulomb barrier of the entrance channels by 4 ~ 7 MeV depending on the systems.

The full width-half-maximum of the barrier distributions, all of Gaussian-like shape, is of the order of 10 ~ 12 MeV and is almost constant for all the systems.

The contribution of the particle transfer channels is shown in the bottom row of Fig. 4 as the ratio of the transfer cross section to the total quasi-elastic one. It is clear that transfer channels give sizable contributions in all the energy range and are the dominant processes at the higher energies. If for quasi-elastic we consider all the final states that belong to the entrance channel mass partition (i.e. only elastic plus inelastic channels) we obtain the quasi-elastic excitation functions and barrier distributions shown with dash-lines in Fig. 4.

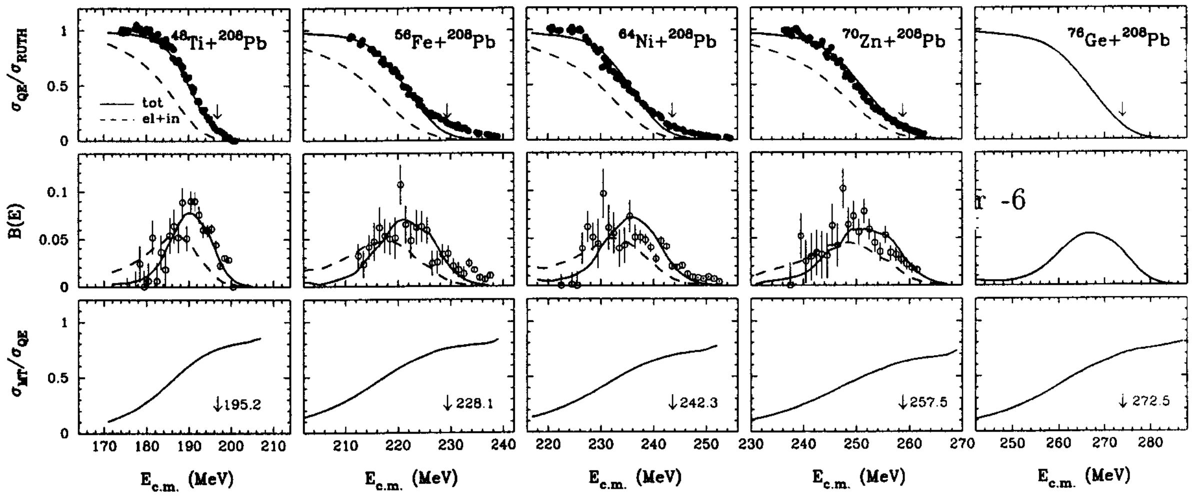

Fig. 4. Quasi-elastic excitation function (top), barrier distribution (middle), ratio of transfer channels to the total quasi-elastic cross section (bottom). All the cross sections have been calculated at $\theta_{lab} = 172^{o}$. The down-arrows represent the Coulomb barrier for the entrance channels calculated with the empirical potential of Ref. [12] and using a two points-charge Coulomb potential. The dash-lines are the results considering as quasi-elastic all the final channels belonging to the entrance channel mass partition. The data are from Ref. [24]

It is clear from the figure that the quasi elastic barrier distribution depends on what we consider quasi-elastic and this make it difficult to have a direct comparison between quasi elastic and fusion barrier distributions, differences may appear due to the different definition of what it is quasi-elastic.

3. Multinucleon transfer reactions and neutron rich heavy nuclei

To estimate the magnitude of a given transfer process it is not necessary to solve explicitly the full system of coupled equations but it sufficies to write down its first order Born approximation. For a given impact parameter (incoming partial wave *l*) the probability for the transition from the entrance channel α to the channel β may be written in the form

$$P_{\beta\alpha}(l) = \left| \frac{i}{\hbar} \int_{-\infty}^{+\infty} dt \; e^{i\sigma_{\beta\alpha} t} f_{\beta\alpha}(0,\vec{r}) e^{i\left[(E_\beta - E_\alpha)t + (\delta_\beta - \delta_\alpha)\right]t/\hbar} \right|^2 , \tag{3}$$

where the time integral has to be performed along the classical trajectory for the given partial wave *l*. In direct processes the two nuclei barely overlap, so that only the tail of the formfactor is relevant. By approximating the true trajectory with a parabolic parametrisation around the turning point the above transition probability may be written in the form

$$P_{\beta\alpha} = \sqrt{\frac{1}{16\pi\hbar^2 |\ddot{r}_0| \kappa_{\alpha_1'}}} \left| f_{\beta\alpha}(0, r_0) \right|^2 g(Q_{\beta\alpha}) , \tag{4}$$

where $\ddot{r}_0$ is the radial acceleration at the distance of closest approach r_0. The adiabatic cut-off function $g(Q)$ is defined as

$$g(Q) = \exp\left(- \frac{(Q - Q_{opt})^2}{\hbar^2 \ddot{r}_0 \kappa_{\alpha_1'}} \right) , \tag{5}$$

where the optimun Q-value is

$$Qopt = \left(\frac{Z_d}{Z_A} - \frac{Z_d}{Z_b} \right) E_B + \left(\frac{m_d}{m_b} - \frac{m_d}{m_A} \right) (E - E_B) + \frac{m_d \ddot{r}_0}{m_a + m_A} (R_A m_b - R_a M_B) \tag{6}$$

and m_d and Z_d are the mass and charge of the transferred particle, E_B is the Coulomb barrier and $\ddot{r}_0$ is the radial acceleration at the distance of closest approach for the grazing partial wave. The adiabatic cut-off function $g(Q)$ defines the actual value of the transition probability, the maximum being at the optimum Q-value. This derives from the requirement that the trajectory of entrance and exit channels matches smoothly close to the turning point where the contribution of the form factor peaks. We notice that the bombarding energy dependence of the cut-off function is contained in the $\ddot{r}_0$ term that defines its width (inversely proportional to the collision time).

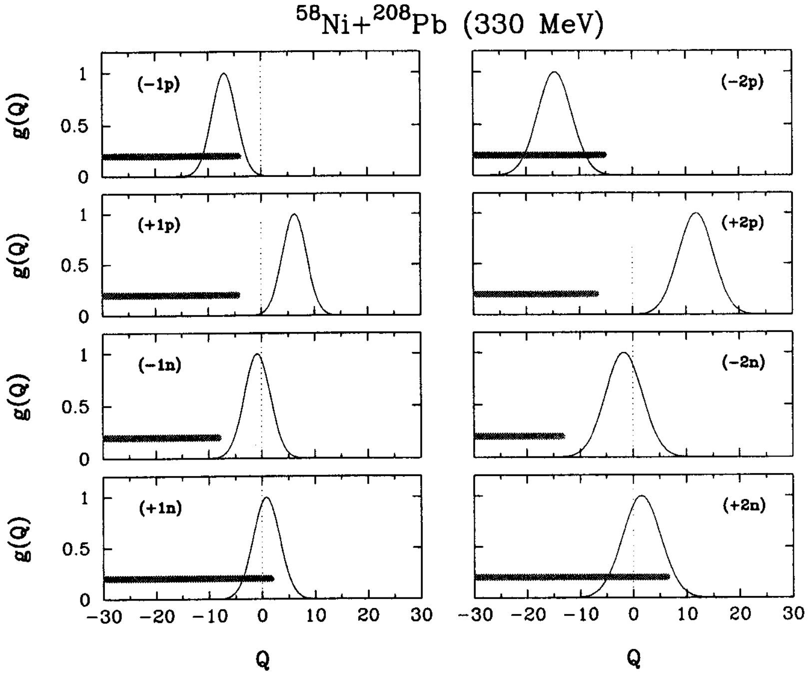

Fig. 5. Adiabatic cut-off functions for one and two neutron and proton transfer channels for the reaction $^{58}Ni + ^{208}Pb$ at the indicated energy. The horizontal lines represent the location of all possible transitions.

In Fig. 5, for the $^{58}Ni + ^{208}Pb$ reaction we show the adiabatic cut-off function g(Q) for all one and two particle transfer channels. In the same figure with horizontal lines we represent, for all channels, the location of all possible transitions. Since only the channels whose Q values lye below the bell shaped curve can actually occur, it is clear that the only allowed transfers are neutron pick-up and proton stripping. All the other channels are hindered by optimun Q-value consideration. From the same figure we notice that for some channels, in particular the two proton stripping and two neutron pick-up, the reaction mechanism favours transitions leading to high excitation energies.

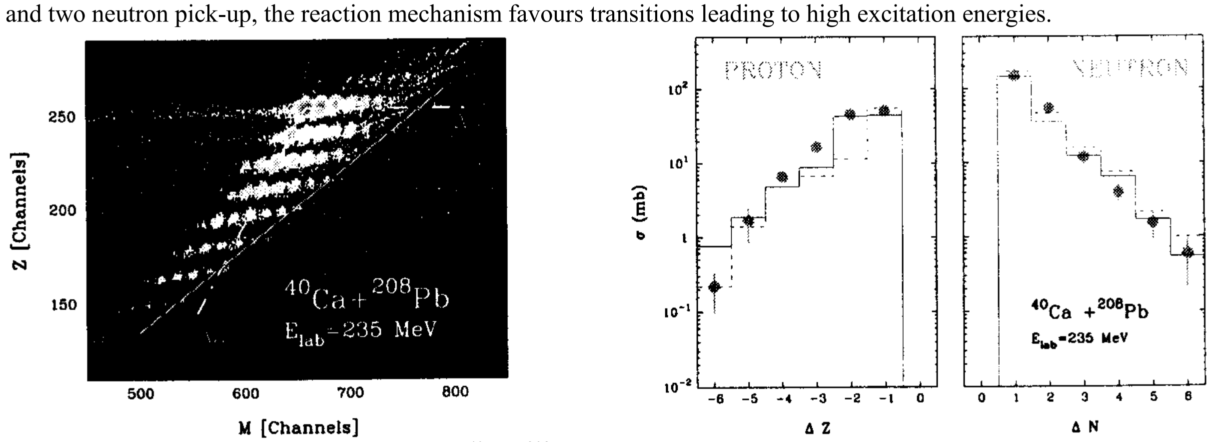

Fig. 6. (left side) Mass-charge distribution of $^{40}Ca+^{208}Pb$ reaction obtained at E_{lab} = 235 MeV and θlab = 84°. The most intense spot corresponds to Z=20 and A=40. Dashed lines correspond to the pure proton stripping (ΔZ) and pure neutron pick-up (ΔN) channels. The full line shows the charge equilibration, namely the N/Z ratio corresponding to the compound. (right side) Angle and Q-value integrated cross sections for pure proton stripping and pure neutron pick-up channels for the same reaction as a function of transferred nucleons. The point and histograms are experimental and theoretical (CWKB) values, respectively. The dashed lines are the results of CWKB using sequential transfer only, while the solid lines include also a pair mode.

Transfer reactions not only give information on how the system dissipates energy and angular momentum from the relative motion to the intrinsic excitation but constitute an important tool for the study of particle correlations in the nuclear media, in particular the one introduced by the paring interaction. To summarize what one has learned [25, 26] in the field of multi-nucleon transfer reactions I will concentrate mostly on the results obtained for the $^{40}Ca + ^{208}Pb$ reaction. In the left-hand side of Fig. 6, *a A - Z* two-dimensional spectrum obtained at E_{lab} = 235 MeV for grazing angle is shown. The dashed lines correspond to pure proton (ΔZ) and pure neutron (ΔN) transfer channels and the full line represents the charge equilibration, namely the location of the *N*/*Z* ratio corresponding to the compound. The final nuclei are all to the left side of this line, indicating the dominance of a direct mechanism where nucleon transfer follows the path expected from optimum *Q*-value arguments that favors neutron pick-up and proton stripping. We notice also that for massive proton transfer channels the isotopic distribution drifts towards lower masses indicating that evaporation processes may play an important role in defining the final isotopic distribution.

The total cross sections, obtained from integrating the angular and *Q*-value distributions for each isotope, are shown for the pure proton stripping and pure neutron pick-up channels to the right-hand side of Fig. 6. The cross sections for the neutron pick-up drop by almost a constant factor for each transferred neutron, as an independent particle mechanism would suggest. The pure proton cross sections behave differently, with the population of the -2*p* channel as strong as the -1*p*. This suggests the contribution of processes involving the transfer of proton pairs in addition to the successive transfer of single protons. The angular distributions are bell shaped indicating that these channels are populated by direct processes.

The total inclusive cross sections for pure neutron and proton channels, obtained when only single-particle transitions are included in the calculations, are shown in Fig. 6 with dash lines. Here the multi-particle transfer channels are reached via a successive mechanism.

As it is seen the theory describes reasonably well the pure neutrons pick-up channels but under-predict considerably the pure two protons stripping channels even if the -1*p* channel is described adequately.

To see if a better description of the data could be obtained, we included pair-transfer modes [27] for proton stripping and neutron pick-up channels (the other two modes, neutron stripping and proton pick-up, may be neglected for *Q*-value reasons). To avoid the use of too many parameters we decided to use only one pair mode for each channel (-2p and +2n) located at optimum *Q*-value (-0.8 MeV for the +2*n* and -17 MeV for the -2*p* channel). The strength of these form factors, kept the same for protons and neutrons, has been fitted to the inclusive cross section of the -2*p* channel obtaining a pair-deformation $\beta_p = 4.3$. The full-line histograms in Fig. 6 represent the results of such calculations. The inclusion of the pair modes is essential for the description of the proton channels and does not alter the good results for the neutron sector.

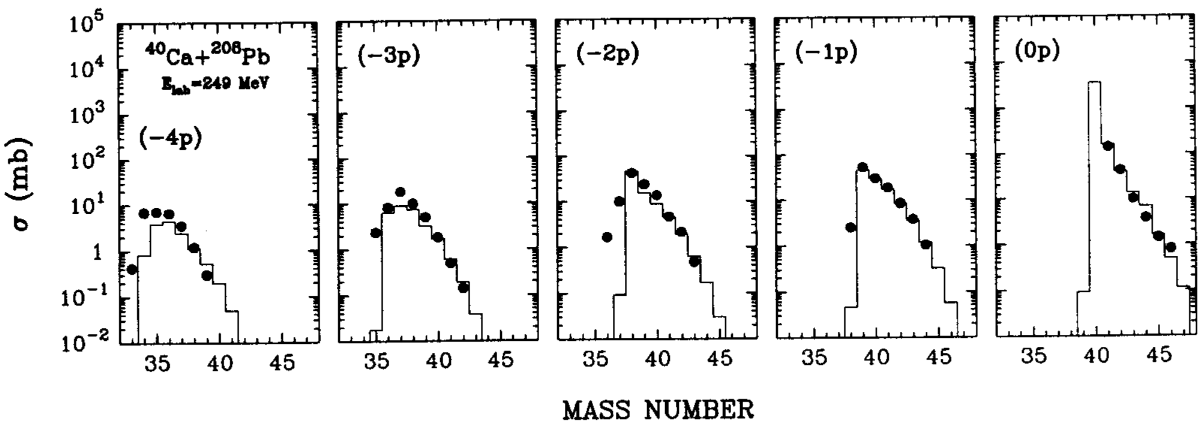

Fig. 7. Total angle and Q-value integrated cross sections for the transfer channels at E_{lab} = 249 MeV. Points and histograms are the experimental and theoretical values, respectively. Experimental errors include the statistical and systematic ones. The calculations include single and pair nucleon transfer modes, and evaporation effects.

For the bombarding energy of 249 MeV we show the full isotopic distribution of the fragments in Fig. 7 in comparison with the data. To obtain this nice description we had to take into account the redistribution of the yields caused by evaporation processes. From the single particle population of the final states we can extract the excitation energy and angular momentum of the fragments, thus by using the code PACE [28] we could estimate the evaporation from the primary fragments. As mentioned above, the inclusion of this process is essential for the description of the yields for the massive charge transfer channels that are shifted towards the lighter masses.

The study of nuclei at the border of the β-stability lines in particular the study of those close to the neutron drip-line constitutes one of the main challenges of the new research with radioactive beams. The production of nuclei close to the proton drip-line does not pose special problems since they can be reached with stable nuclei via fusion reactions or via fragmentation. Unfortunately these kinds of techniques do not work for the production of heavy neutron rich nuclei. These can eventually be produced or via spallation reactions with energetic proton beams or via very asymmetric fission reactions. In the following I will try to convince you that multinucleon transfer reactions can offer an alternative mechanism for the production of these heavy neutron rich nuclei.

By looking at the chart of nuclei it is clear that one should be able to reach the region of neutron reach heavy nuclei just by extracting protons (i.e making protons pick-up reactions) from a heavy stable targets or transferring some neutrons (i.e. making neutron stripping reactions). Unfortunately proton pick-up and neutron stripping are very weak reactions when stable nuclei are involved thus one has to resort to the use of neutron rich projectile as was discussed in Refs. [29, 30].

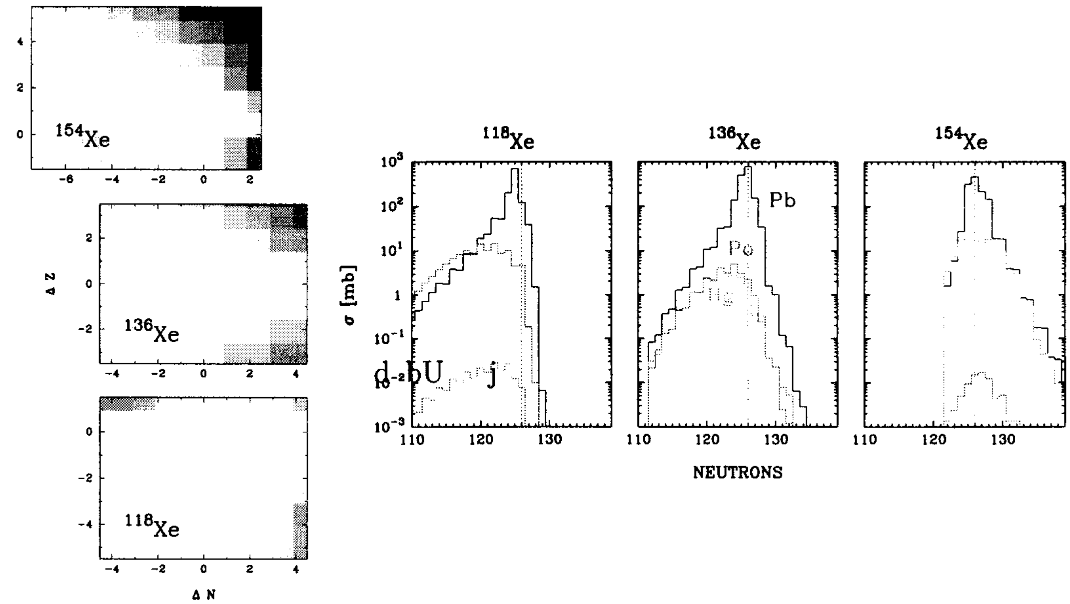

Fig. 8. Total angle and Q-value integrated cross sections for the transfer channels at E_{lab} = 249 MeV. Points and histograms are the experimental and theoretical values, respectively. Experimental errors include the statistical and systematic ones. The calculations include single and pair nucleon transfer modes, and evaporation effects.

Focusing in the region of the nuclei chart close to the magic number *N*=126 we show on the left hans side of Fig. 8 how multinucleon transfer reactions on ^{208}Pb evolve by using, are projectile, several isotopes of xeon. It is clear from the figure that with neutron-rich projectile the population evolves toward proton pick-up thus populating nulei below the lead.

This is particular evident by applying cuts on the double differential cross section. These cuts are shown on the right-hand-side of the same figure where the production of mercury (+2*p* channels) and polonium (-2*p* channels) isotopes is compared for the different xeon isotopes, the bombarding energy is set at 700 MeV in the center-of-mass system for all the systems. The advantage of the neutron rich xeon in clear in fact with this projectile one can populate, with reasonable cross section, isotope well outside the last synthesized up to now. Quite interestingly one should notice that the cross sections have almost an exponential decay as a function of the neutron number. One loses a factor 3 - 4 in the cross section for each transferred neutron.

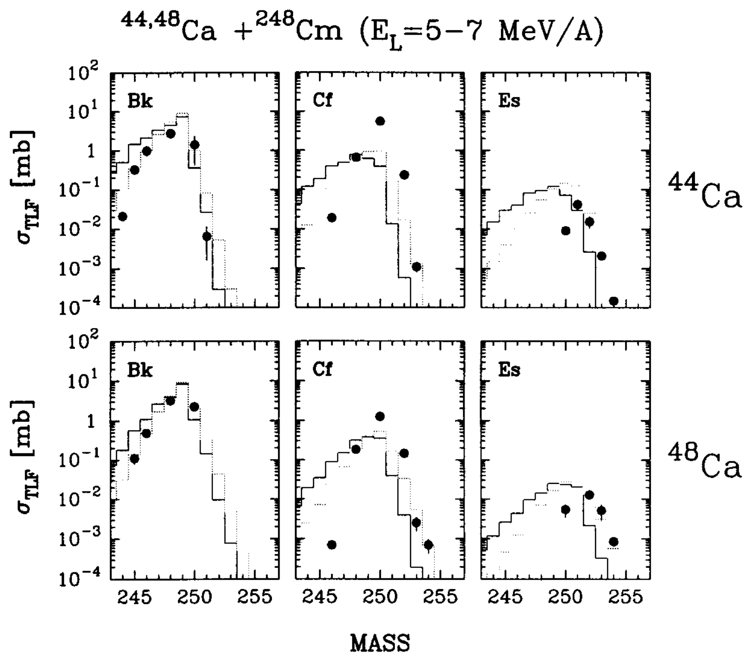

Fig. 9. Production of the indicated heavy actinide in the collision with ^{248}Cm in comparison with the experimental data. The results of the calculation have been scaled down by a factor 5 to take into account (in a very qualitative way) the fission probability of the heavy reaction products.

In the past there has been a great deal of interest [31, 32] in the use of heavy-ion transfer reactions with actinide targets to produce new nuclear species in the actinide and transactinide region. In Fig. 9 are shown some of the results obtained from the collision of ^{44}Ca and ^{48}Ca on ^{248}Cm at energies close to the Coulomb barrier. Here we focus on reaction products with nuclear charges in excess of that of the target since with stable beam only proton stripping reactions are possible. In the same figure, with hystograms, are also reported the results obtained with GRAZING, to take into account the fission of the reaction products tha theoretical calculations have been scaled down by a factor of 5. The two histograms are reported to indicate the uncertainties introduced due to neutron evaporation. The comparison has to be considered only qualitative because of the many uncertainties involved; of course one can not use a single parameter to scale the cross section for all the nuclear species since the fission probability thus depend from nucleus to nucleus. Nevertheless it is quite interesting to note that the relative population of the different isotopes is quite well reproduced.

4. Conclusions

The semi-classical theory offers a very powerful tool for the analysis of heavy-ion reactions. It allows a clear separation between the relative motion variables and the intrinsic degrees of freedom, surface vibrations and particle transfer. The role of these two classes of degrees of freedom may be easily discussed. While capture cross section is dominated by the dynamics of the nuclear surfaces the transfer channels acting mostly as absorber of the entrance flux.

REFERENCES

1. *Gross D.H.E., Kalinowski H.* // Phys. Lett. - 1974. - Vol. B48. - P. 302.
2. *Randrup J., Swiatecki W.J.* // Ann. Phys. (N.Y.) - 1980. - Vol. 125. - P. 193; Nucl. Phys. - 1984. - Vol. A429. - P. 105.
3. *Esbensen H.* // Nucl. Phys. 1981. - Vol. A352. - P. 147.
4. *Rowley N., Satchler G.R., Stelson P.H.*
5. *Broglia R.A., Pollarolo G., Winther A.* // Nucl. Phys. - 1981. - Vol. A361. - P. 307.
6. *Pollarolo G., Broglia R.A., Winther A.* // Nucl. Phys. -1983. - Vol. A406. - P. 369.
7. *Thompson I.J., Nagarajan M.A., Lilley J.S., Fulton B.R.* // Phys. Lett. - 1985. - Vol. B157. - P. 250.
8. *Winther A.* // Nucl. Phys. - 1994. - Vol. A572. - P. 191.
9. *Winther A.* // Nucl. Phys. - 1995. - Vol. A594. - P. 203.
10. Pollarolo G., Winther A. // Pys. Rev. - 2000. - Vol. C62. - P. 054611.
11. *Winther A.* GRAZING, computer program. (may be downloaded from: http : //www.to.infn.it/ ~ nanni/grazing).
12. *Broglia R., Winther A.* Heavy Ion Reactions. - Redwood City CA: Addison-Wesley Pub. Co., 1991.
13. *Quesada J.M., Pollarolo G., Broglia R.A., Winther A.* // Nucl. Phys. - 1985. - Vol. A442. - P. 381.
14. *Freeman W.S. et al.* // Phys. Rev. Lett. - 1983. - Vol. 50. - P. 1563.
15. *Lesko K.T. et al.* // Phys. Rev. Lett. - 1985. - Vol. 55. - P. 803; Phys. Rev. - 1986. - Vol. C34. - P. 2155.
16. *Wolf F.L.H. et al.* // Phys. Lett. - 1987. - Vol. B196. - P. 113.
17. *Wolf F.L.H.* // Phys. Rev. - 1987. - Vol. C36. - P. 1379.
18. *Betts R.R. et al.* // Phys. Rev. Lett. - 1987. - Vol. 59. - P. 978.
19. *Pass C.N. et al.* // Nucl. Phys. - 1989. - Vol. A499. - P. 173.
20. *Henning W. et al.* // Phys. Rev. Lett. - 1987. - Vol. 58. - P. 318.
21. *Van den Berg A.M. et al.* // Phys. Rev. Lett. - 1986. - Vol. 56. - P. 572; Phys. Rev. - 1988. - Vol. C37. - P. 178.
22. *Jiang C.L. et al.* // Phys. Rev. - 1998. - Vol. C57. - P. 2383.
23. *Esbensen H., Jiang C.L., Rehm K.E.* // Phys. Rev. - 1998. - Vol. C57. - P. 2401.
24. *Mitsuoka S., Ikezoe H., Nishio K. et al.* // Phys. Rev. Lett. - 2007. - Vol. 99. - P. 182701.
25. *Szilner S., Corradi L., Haas F. et al.* // Eur. Phys. J. - 2004. - Vol. A21. - P. 87.
26. *Szilner S., Corradi L., Pollarolo G. et al.* // Phys. Rev. - 2005. - Vol. C71. - P. 044610.
27. *Dasso C.H., Pollarolo G.* // Phys. Lett. - 1985. - Vol. 155B. - P. 223.
28. *Gavron A.* // Phys. Rev. - 1980. - Vol. C21. - P. 230.
29. *Dasso C.H., Pollarolo G., Winther A.* // Phys. Rev. Lett. - 1995. - Vol. 73. - P. 1907.
30. *Dasso C.H., Pollarolo G., Winther A.* // Phys. Rev. - 1995. - Vol. C52. - P. 2264.
31. *Schädel M., Brüchle W., Gäggeler H. et al.* // Phys. Rev. Lett. - 1982. - Vol. 48. - P. 852.
32. *Hoffman D.C., Fowler M.M., Daniels W.R. et al.* // Phys. Rev. - 1985. - Vol. C31. - P. 1763.